REPORT DOCUMENTATION PAGE

[1] Form Approved OMB NO. 0704-0188

1. REPORT DATE (DD-MM-YYYY)	2. REPORT TYPE	3. DATES COVERED (From - To)
	New Reprint	-

4. TITLE AND SUBTITLE
Incorporation kinetics in mixed anion compound semiconductor alloys

5a. CONTRACT NUMBER
W911NF-12-1-0338

5b. GRANT NUMBER

5c. PROGRAM ELEMENT NUMBER
611102

6. AUTHORS
Joanna M. Millunchick, Evan M. Anderson, Chris Pearson, Wendy L. Sarney, Stefan P. Svensson

5d. PROJECT NUMBER

5e. TASK NUMBER

5f. WORK UNIT NUMBER

7. PERFORMING ORGANIZATION NAMES AND ADDRESSES
University of Michigan - Ann Arbor
3003 S. State St
Ann Arbor, MI 48109 -1274

8. PERFORMING ORGANIZATION REPORT NUMBER

9. SPONSORING/MONITORING AGENCY NAME(S) AND ADDRESS (ES)
U.S. Army Research Office
P.O. Box 12211
Research Triangle Park, NC 27709-2211

10. SPONSOR/MONITOR'S ACRONYM(S)
ARO

11. SPONSOR/MONITOR'S REPORT NUMBER(S)
60729-MS.5

12. DISTRIBUTION AVAILIBILITY STATEMENT
Approved for public release; distribution is unlimited.

13. SUPPLEMENTARY NOTES
The views, opinions and/or findings contained in this report are those of the author(s) and should not contrued as an official Department of the Army position, policy or decision, unless so designated by other documentation.

14. ABSTRACT
We present a kinetic model predicting anion incorporation in InAsSb. Included are the effects of As desorption, Sb segregation, and Sb displacement by As, any of which may be limited by the In flux if it is comparatively larger. The model captures experimental data over a range of growth conditions for the InAsSb system using activation energies for desorption and Sb segregation found in literature. The activation energy for Sb displacement found in this work is 1.3 eV. This model is general and should be valid for other mixed anion systems, or, appropriately modified, mixed cation systems and mixed anion/cation systems such as AlInAsSb.

15. SUBJECT TERMS
Sb incorporation, kinetic model, molecular beam epitaxy, surface segregation

16. SECURITY CLASSIFICATION OF:			17. LIMITATION OF ABSTRACT	15. NUMBER OF PAGES	19a. NAME OF RESPONSIBLE PERSON
a. REPORT	b. ABSTRACT	c. THIS PAGE			Joanna Millunchick
UU	UU	UU	UU		19b. TELEPHONE NUMBER 734-647-8980

Report Title

Incorporation kinetics in mixed anion compound semiconductor alloys

ABSTRACT

We present a kinetic model predicting anion incorporation in InAsSb. Included are the effects of As desorption, Sb segregation, and Sb displacement by As, any of which may be limited by the In flux if it is comparatively larger. The model captures experimental data over a range of growth conditions for the InAsSb system using activation energies for desorption and Sb segregation found in literature. The activation energy for Sb displacement found in this work is 1.3 eV. This model is general and should be valid for other mixed anion systems, or, appropriately modified, mixed cation systems and mixed anion/cation systems such as AlInAsSb.

REPORT DOCUMENTATION PAGE (SF298)
(Continuation Sheet)

Continuation for Block 13

ARO Report Number 60729.5-MS
Incorporation kinetics in mixed anion compound...

Block 13: Supplementary Note

Approved for public release; distribution is unlimited.

Incorporation Kinetics in Mixed Anion Compound Semiconductor Alloys

Joanna M. Millunchick and Evan M. Anderson, Department of Materials Science and Engineering, University of Michigan, Ann Arbor, MI 48109

Chris Pearson, Department of Computer Science, Engineering, and Physics, University of Michigan–Flint, Flint, MI 48502

Wendy L. Sarney and Stefan P. Svensson, Army Research Laboratory, 2800 Powder Mill Rd, Adelphi, MD 20783

Abstract

We present a kinetic model predicting anion incorporation in InAsSb. Included are the effects of As desorption, Sb segregation, and Sb displacement by As, any of which may be limited by the In flux if it is comparatively larger. The model captures experimental data over a range of growth conditions for the InAsSb system using activation energies for desorption and Sb segregation found in literature. The activation energy for Sb displacement found in this work is 1.3eV. This model is general and should be valid for other mixed anion systems, or, appropriately modified, mixed cation systems and mixed anion/cation systems such as AlInAsSb.

Since the invention of the MBE technology, most work on alloys with three or more constituents has focused on mixed Group-III materials. This has enabled the development of a wide range of important semiconductor heterostructures and devices. Alloying the Group-III elements was a natural beginning for the technology due to the relatively straight-forward composition control allowed: under most typical growth conditions the Group-III elements add linearly to the total growth rate and the resulting composition is directly obtained as a ratio of the individual rates. In contrast, mixed anion (Group-V) alloys are more complex to control. The Group-V elements usually do not influence the growth rates, and the resulting composition is not merely the ratio of the fluxes. Instead, there are many competing processes that alter the incorporation rates of these elements. However, mixed Group-V alloys offer many new important materials properties that are not possible with Group-III alloys and are therefore of interest to explore. Examples are dilute bismuthides [1] and nitrides [2] that can produce reduced bandgaps while remaining lattice matched to available substrates, and the emerging field of highly-mismatched alloys such as dilute-antimonide GaNSb [3] and very narrow bandgap materials such as InAsSb, which is the main focus of this work.

Mixed As/Sb alloys have been produced for several decades.[4] The properties of MBE-grown InAsSb in particular has been studied. [5-8] but few reports attempting to systematically determine the Sb/As incorporation as a function of growth parameters exist other than some empirical work. [9,10] It has recently been demonstrated that InAsSb has a smaller bandgap than previously thought. [11,12] This opens up a long sought path to a III-V, direct-bandgap, long-wavelength, infrared detector material that can rival HgCdTe without the complications and drawbacks associated with superlattices.[13] In order to produce such material, it needs to be grown strain-free so that the resulting bandgap is not affected by residual strain or Group-V sublattice ordering, and the composition of the alloy needs to be well controlled so that the bandgap targeted for specific device applications is obtained.[14] Further materials optimization requires variations of the growth conditions, while maintaining a desired target composition. It is therefore of great

importance to be able to model the incorporation process to guide and reduce the number of optimization experiments.

Typically, any general kinetic model takes into account all of the physical processes that take place during growth. Many such models have been developed for the mixed anion alloys, including GaAsP [15], GaAsSb [16], and GaAsBi [17]. No modeling of the growth of InAsSb is available in the literature, however. Here we present a model that addresses incorporation in unstrained material taking into account desorption, Sb segregation and As displacement of Sb and apply it to InAsSb. The only fitting parameter of the resulting model is the activation energy of As displacement, which was found to be 1.3 eV. The model fits agree well with experimental results obtained in multiple laboratories, and provide the sought after ability to predict the Sb composition from known experimental parameters.

Kinetic model

In this general kinetic model, we consider the incorporation of elements into a compound $MA_{1-x}S_x$, where M is the Group-III metal, A is the Group-V anion, and S is the Group-V segregant, that is, the element that is more easily displaced in the alloy (eg: Sb in $InAs_{1-x}Sb_x$ or Bi in $GaAs_{1-x}Bi_x$). We are interested in understanding how the concentration of the segregant in the bulk x_b changes as a function of growth parameters such as temperature T, flux of the segregant F_s, flux of the anion F_a, and flux of the metal F_m. We do this by taking into account all of the processes that affect the coverage of each of the constituents. The composition of the segregant at the surface x_s is a ratio of the coverage of each species in the following manner:

$$x_s = \theta_s / (\theta_s + \theta_a) \qquad (1)$$

where θ is the surface coverage of the anion and segregant respectively. x_b and x_s are not necessarily the same value due to surface segregation, as will be discussed below.

Several processes have been identified that affect the amount of each species, as shown in Fig. 1. The incident flux is the primary term, but this contribution is reduced in the presence of desorption. Surface segregation, or the exchange of a surface anion species with a subsurface segregant species, is also well known for a number of mixed anion alloys such as GaAsSb, GaSbBi, and InAsSb. Both Sb and Bi have been reported to be excellent surfactants, remaining primarily on the surface rather than incorporating into the film under the appropriate growth conditions. [18] [19]It has also been reported in some mixed anion alloys that one species may displace the other. For instance, it has been shown that the incorporation of Sb in GaAsSb is hampered in the presence of a large As flux, [9] however, this effect has not been reported for InAsSb.

The rate of desorption, displacement, and segregation are activated processes, and have a strong dependence on temperature with the standard Arrhenius form:

$$P_i = N\nu exp\left(-\frac{E_i}{kT}\right) \qquad (2)$$

Where N is the number of atomic sites on the surface, ν is the attempt frequency $4x10^{12}$ s^{-1} , E_i is the activation energy of the ith process, k is Boltzmann's constant, and T is the temperature. It is also possible to include terms for the formation of metal or segregant droplets, which has been observed in growth with Sb [20] and Bi,[21] but for the purpose of this work we will only consider anion overpressures for which droplets are not expected to form. In this case, the surface is always covered in either the anion or segregant such that $\theta_s + \theta_a = 1$.

The rate of each process is not the only factor that needs to be included. The form of each term must also include a limiting factor ϕ_{ij} that takes into account the fact that deposition of another species, F_j, may limit the process in question:

$$\phi_{ij} = \frac{P_i}{P_i + F_j} \qquad (3)$$

ϕ_{ij} approaches unity when the reaction rate is fast compared to the arrival of the

species that would prevent the reaction from taking place, and zero when the reaction rate is slow in comparison. In the experiments that follow, the limiting flux is always that of the metal, thus we simplify the notation for the limiting factor to ϕ_i.

The fact that there is surface segregation implies that there is a difference between the composition at the surface x_s and in the bulk x_b. The bulk composition is proportional to the surface composition via the equilibrium partition coefficient K, which is the fraction of the segregant that remains in the film.[22] The value of K can range from 0 (for a pure surfactant) to 1 (for complete incorporation). That coefficient may be modified via the ratio of the rate of the segregation P_{seg} and the rate of the arrival of the metal, F_m, that frustrates the segregation. The form is such that the effective coefficient goes to K when F_m is small compared to P_{seg}, and unity when it is large. Thus the composition of the bulk is the product of the surface concentration and the effective segregation parameter:

$$x_b = x_s \frac{K + {F_m}/{P_{seg}}}{1 + {F_m}/{P_{seg}}} \qquad (4)$$

The growth rate of the segregant is given by:

$$J_s = F_s - \theta_s P_{sdes} \phi_{sdes} + x_b \theta_a P_{seg} \phi_{seg} - \theta_s P_{dis} \phi_{dis} \qquad (5)$$

The first term on the right hand side represents the amount of impinging material, F_s. The second term represents the reduction in the net flux due to desorption, which is the product of the rate of desorption and the limiting factor comparing the desorption rate and the arrival of the metal. The third term increases the net flux via surface segregation, which is the product of the rate of segregation and the limiting factor comparing the desorption rate and the arrival of the metal. The fourth term reduces the net flux as a result of anion displacement, which is the product of the rate of displacement and the limiting factor comparing the desorption rate and the arrival of the metal. The growth rate of the anion species may be written in a similar manner, with the exception of terms 3 and 4, which describe reaction rates between the anion and segregant. The displacement term is the same for both equations,

except that this term acts to increase the anion growth rate. The segregation term, on the other hand, acts to decrease the anion growth rate. These equations can be solved simultaneously to determine x_b as a function of the growth parameters.

Experimental Data

Several $InAs_{1-x}Sb_x$ samples were grown with two MBE systems in our respective laboratories and compared to the predictions of the kinetic model. All samples were growth using solid sources for Group-III and valved sources with cracking zones for As and Sb. ARL samples were grown with a residual strain less than 0.1% on graded buffer layers as described earlier [23] at a substrate temperature of 415 C, measured with a K-space BandIT system operated in pyrometry mode and calibrated with a blackbody source through the heated viewport. The emissivity was set to produce the characteristic RHEED pattern transition on GaSb from x3 to x5 at 430 C. [24]

Absolute flux values were determined in two different ways. In the first case we started by measuring the growth rates with RHEED oscillations under excess group V flux, which allowed us to relate the group III BEP to flux. We then reduced the group V flux until we observed a reduction in the growth rate, at which point we assumed that the group III and V fluxes were equal. In the second case, flux was determined by monitoring the RHEED pattern until it changed from a group V terminated surface to a group III terminated surface. This point was taken to correspond to a V/III ratio of 1. Because the group III growth rate is not influenced by desorption or any other depleting processes, the RHEED calibrated rate can be assumed to be equivalent to its flux as measured by a Beam Flux Monitor. After taking into account beam flux monitor sensitivities, the In flux is assumed to be equal to the anion flux at V/III=1. The procedure was done for both anions. UM samples were grown over a range of In rates using different temperatures, as measured using a low temperature pyrometer. Film growth was monitored *in situ* using RHEED and *ex situ* using high-resolution x-ray diffraction. The Sb-

composition values were obtained from XRD data using symmetric (004) scans and asymmetric (115) scans.

Figure 2 shows the bulk composition x_b of nearly lattice matched InAsSb/GaSb as a function of growth temperature T and In growth rate F_m. The data exhibits a small negative slope for each set of data at a constant growth rate, and increasing bulk composition with increasing Fm. Figure 2 also shows the fit to the data using the kinetic model using activation energies for the desorption and segregation found in the literature (shown in Table 1). The segregation energy calculated from reference [25] is 1.2 eV, and the segregation parameter is 0.4. The activation energy for As displacement of Sb was a fitting parameter, and was found to be 1.3 eV. The fit shows that the temperature dependence of the composition is not a simple Arrhenius, but instead depends on the interplay between the different terms. In these experiments, the desorption rates are slow and don't contribute much to the fluxes and thus to the composition. Both the segregation and displacement terms act to reduce the composition as long as Fm is low. Since the activation energy to segregate is lower than to displace Sb, segregation is the dominant mechanism that reduces composition at low temperature. Assuming only segregation the composition will increase with increasing temperature until it reaches the equilibrium composition, 0.4. The fact that lower compositions are observed suggest that the rate of displacement of Sb by As becomes appreciable at higher temperatures, which reduces the coverage of Sb on the surface and thus the amount of Sb that may incorporate into the film.

The fact that the composition increases with increasing In flux is evident from the data. The model also predicts this trend. An increase in F_m increases the amount of Sb incorporation. Inspection of equation 3 shows that an increase in F_m will result in a decrease of the efficiency factor ϕ for both the As displacement and Sb surface segregation. Both of these effects lead to more Sb incorporation. Furthermore, higher F_m will result in an increase in the segregation coefficient (equ. 4). All of these indicate that increasing F_m will result in the kinetic trapping of the segregant. The desorption rates for As and Sb are slow for InAsSb, [26,27] typically

less than the arrival rate of In, so that these terms have a negligible impact on the F_m dependence of the composition.

The plots in Fig. 3 demonstrate the dependence of the bulk composition as a function of group III and V fluxes. Fig. 3a shows the Sb/As flux ratio at the growth temperature of 415 C. The points of the same color are those for which the As flux was varied and the In and Sb were held nominally constant. The experimental data shows that the composition increases sublinearly with increasing Sb/As. The solid lines show the fits of the model to the data using the parameters listed in Table 1. The model predicts that there is a dependence on the absolute In, Sb, or As flux on the composition as a function of Sb/As flux ratio, in agreement with results shown for GaAsSb.[9] The amount of Sb incorporation increases with lower absolute Sb flux, presumably because the As displacement is lower. The model also predicts that the absolute fluxes influence the composition as a function of V/III ratio, shown in Fig. 3b. The composition decreases with V/III ratio when holding the Sb and In fluxes constant. The magnitude of the composition depends on the absolute value of the Sb (As) flux, with higher Sb (As) flux resulting in a higher (lower) incorporation of Sb. This also supports the observation that the As displacement mechanism is offset (enhanced) by the higher flux of Sb (As).

Figure 4 shows a map that plots the growth conditions to obtain particular compositions for an In flux of 6.3×10^{18}, corresponding to 1 um/hr, and growth temperatures of 405, 415, and 425. The limit on the y-axis does not go to zero, because ratios less than 1 indicate that the surface is metal terminated, conditions for which this model is not valid. The contours from left to right represent the conditions for $0.1 \leq x \leq 0.4$. The composition varies weakly as a function of the V/III ratio at low Sb/As ratio, but increases in sensitivity as the Sb/As ratio increases. Similarly, the composition is weakly affected at low Sb/As ratios and more strongly at higher ratios. Both of these facts arise because the interaction between the Sb segregation and the As displacement becomes stronger as the absolute amount of both anion fluxes increases.

Conclusions

We have shown that a relatively simple model can well describe the qualitative and quantitative incorporation of As and Sb in InAsSb. Both As displacement and Sb segregation result in a depletion of Sb in the film. The activation energy for As displacement of Sb is found to be 1.3 eV. Any of these processes may be limited by the In flux, which will inhibit that process if it is larger than the process rate, however, this has a relatively small affect. A growth condition map was also generated that provides valuable guidance on how to achieve compositional control of this difficult to grow alloy. This model is completely general and should also be valid for other mixed anion systems, including those with phosphorous or bismuth. Furthermore, the model may be easily modified to examine mixed cation alloys where one cation acts as a segregant, or even mixed anion/mixed cation systems such as AlInAsSb.

Acknowledgement

JMM, EMA, and CP gratefully acknowledge Chakrapani Varanasi and the support of the Department of Defense, Army Research Office via the grant number W911NF-12-1-0338 .

References

[1] T. Tiedje, E.C. Young, and A. Mascarenhas, … Journal of Nanotechnology (2008).

[2] J.N. Beaudry, R.A. Masut, and P. Desjardins, J Cryst Growth **310**, 1040 (2008).

[3] S.V. Novikov, K.M. Yu, A. Levander, D. Detert, W.L. Sarney, Z. Liliental-Weber, M. Shaw, R.W. Martin, S.P. Svensson, W. Walukiewicz, and C.T. Foxon, J Vac Sci Technol B **31**, 03C102 (2013).

[4] C.A. Chang, R. Ludeke, L.L. Chang, and L. Esaki, Appl Phys Lett **31**, 759 (1977).

[5] M.Y. Yen, R. People, K.W. Wecht, and A.Y. Cho, Appl Phys Lett **52**, 489 (1988).

[6] I.T. Ferguson, A.G. Norman, B.A. Joyce, T.Y. Seong, G.R. Booker, R.H. Thomas, C.C. Phillips, and R.A. Stradling, Appl Phys Lett **59**, 3324 (1991).

[7] S.R. Kurtz, L.R. Dawson, R.M. Biefeld, D.M. Follstaedt, and B.L. Doyle, Physical Review B **46**, 1909 (1992).

[8] T.Y. Seong, G.R. Booker, A.G. Norman, and I.T. Ferguson, Appl Phys Lett **64**, 3593 (1994).

[9] A. Bosacchi, S. Franchi, P. Allegri, V. Avanzini, A. Baraldi, R. Magnanini, M. Berti, D. De Salvador, and S.K. Sinha, J Cryst Growth **201**, 858 (1999).

[10] X. Marcadet, A. Rakovska, I. Prevot, G. Glastre, B. Vinter, and V. Berger, J Cryst Growth **227**, 609 (2001).

[11] Y. Lin, D. Wang, D. Donetsky, L. Shterengas, G. Kipshidze, G. Belenky, S.P. Svensson, W.L. Sarney, and H.S. Hier, J Electron Mater **42**, 918 (2013).

[12] S.P. Svensson, W.L. Sarney, H. Hier, Y. Lin, D. Wang, D. Donetsky, L. Shterengas, G. Kipshidze, and G. Belenky, Physical Review B **86**, (2012).

[13] S.P. Svensson, D. Donetsky, D. Wang, H. Hier, F.J. Crowne, and G. Belenky, J Cryst Growth **334**, 103 (2011).

[14] G. Belenky, D. Donetsky, G. Kipshidze, D. Wang, L. Shterengas, W.L. Sarney, and S.P. Svensson, Appl Phys Lett **99**, (2011).

[15] B.W. Liang and C.W. Tu, J Appl Phys **74**, 255 (1993).

[16] J.-M. Lin, L.-C. Chou, and H.-H. Lin, J Vac Sci Technol B **29**, 021011 (2011).

[17] X. Lu, D. Beaton, R. Lewis, T. Tiedje, and M. Whitwick, Appl Phys Lett **92**, 192110 (2008).

[18] J.K. Shurtleff, R.T. Lee, C.M. Fetzer, and G.B. Stringfellow, Appl Phys Lett **75**, 1914 (1999).

[19] M. Pillai, S. Kim, S. Ho, and S. Barnett, J Vac Sci Technol B **18**, 1232 (2000).

[20] T. Kawazu, T. Mano, T. Noda, Y. Akiyama, and H. Sakaki, Phys Status Solidi B **246**, 733 (2009).

[21] M. Masnadi-Shirazi, D.A. Beaton, R.B. Lewis, X.F. Lu, and T. Tiedje, *Surface Reconstructions During Growth of $GaAs_{1-X}Bi_X$ Alloys by Molecular Beam Epitaxy* (n.d.).

[22] J.Y. Tsao, *Materials Fundamentals of Molecular Beam Epitaxy* (Academic Press, Boston, 1993).

[23] G. Belenky, D. Wang, Y. Lin, D. Donetsky, G. Kipshidze, L. Shterengas, D. Westerfeld, W.L. Sarney, and S.P. Svensson, Appl Phys Lett **102**, 111108 (2013).

[24] A. Bracker, M. Yang, B. Bennett, J. Culbertson, and W. Moore, J Cryst Growth **220**, 384 (2000).

[25] A. Semenov, O.G. Lyublinskaya, V.A. Solov'ev, B.Y. Meltser, and S.V. Ivanov, J Cryst Growth **301-302**, 58 (2007).

[26] A.J. Noreika, M.H. Francombe, and C.E.C. Wood, J Appl Phys **52**, 7416 (1981).

[27] B.W. Liang and C.W. Tu, J Cryst Growth **128**, 538 (1993).

Table 1: Parameters used to fit the model to the experimental data.

Desorption Energy of As from InAs	2.4 eV	Reference [27]
Desorption Energy of Sb from InSb	2.7 eV	Reference [26]
Segregation Energy of Sb in InAsSb	1.2 eV	Reference [25]
Equilibrium segregation parameter	0.4	Reference [25]
Energy for As displacement of Sb in InAsSb	1.3 eV	this work

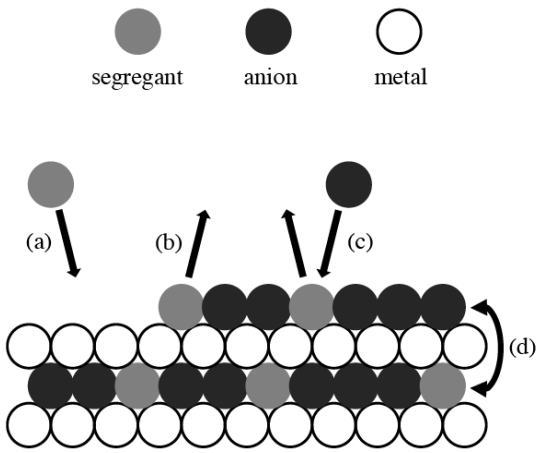

Figure 1: Factors governing the surface coverage include (a) deposition, (b) desorption, (c) displacement, and (d) segregation.

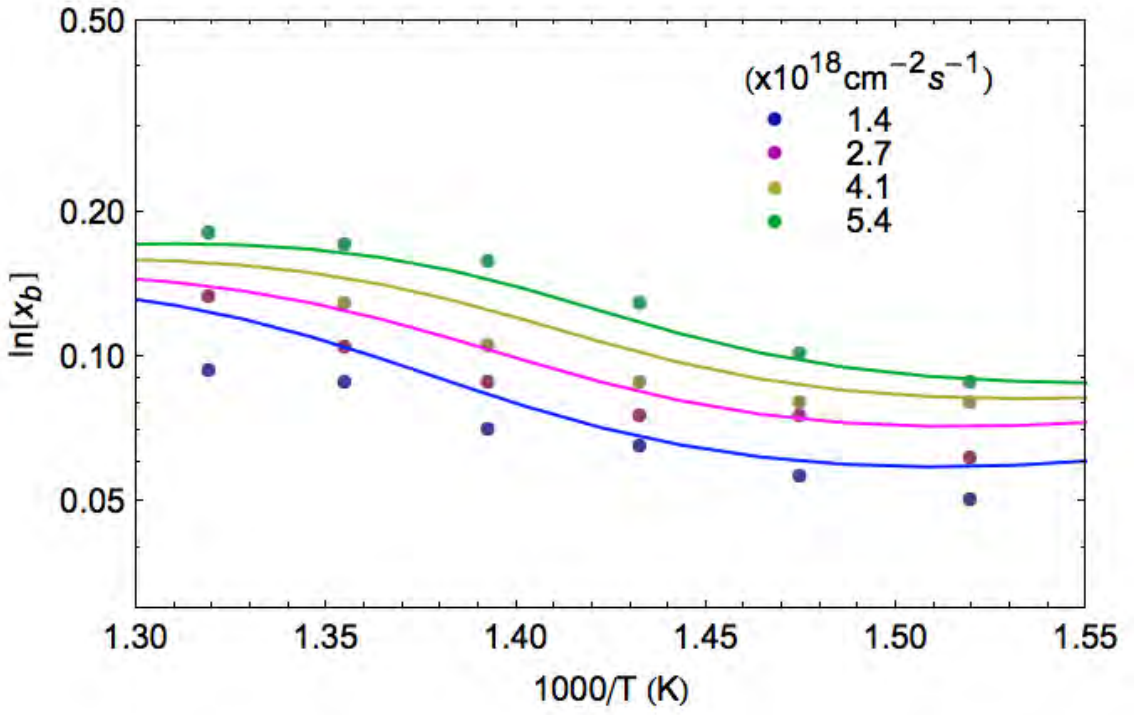

Figure 2: Sb bulk concentration as a function of inverse temperature for In fluxes $1<F_m<5.5x10^{18}$ $cm^{-2}s^{-1}$. The solid lines are the model fit using the parameters in Table 1

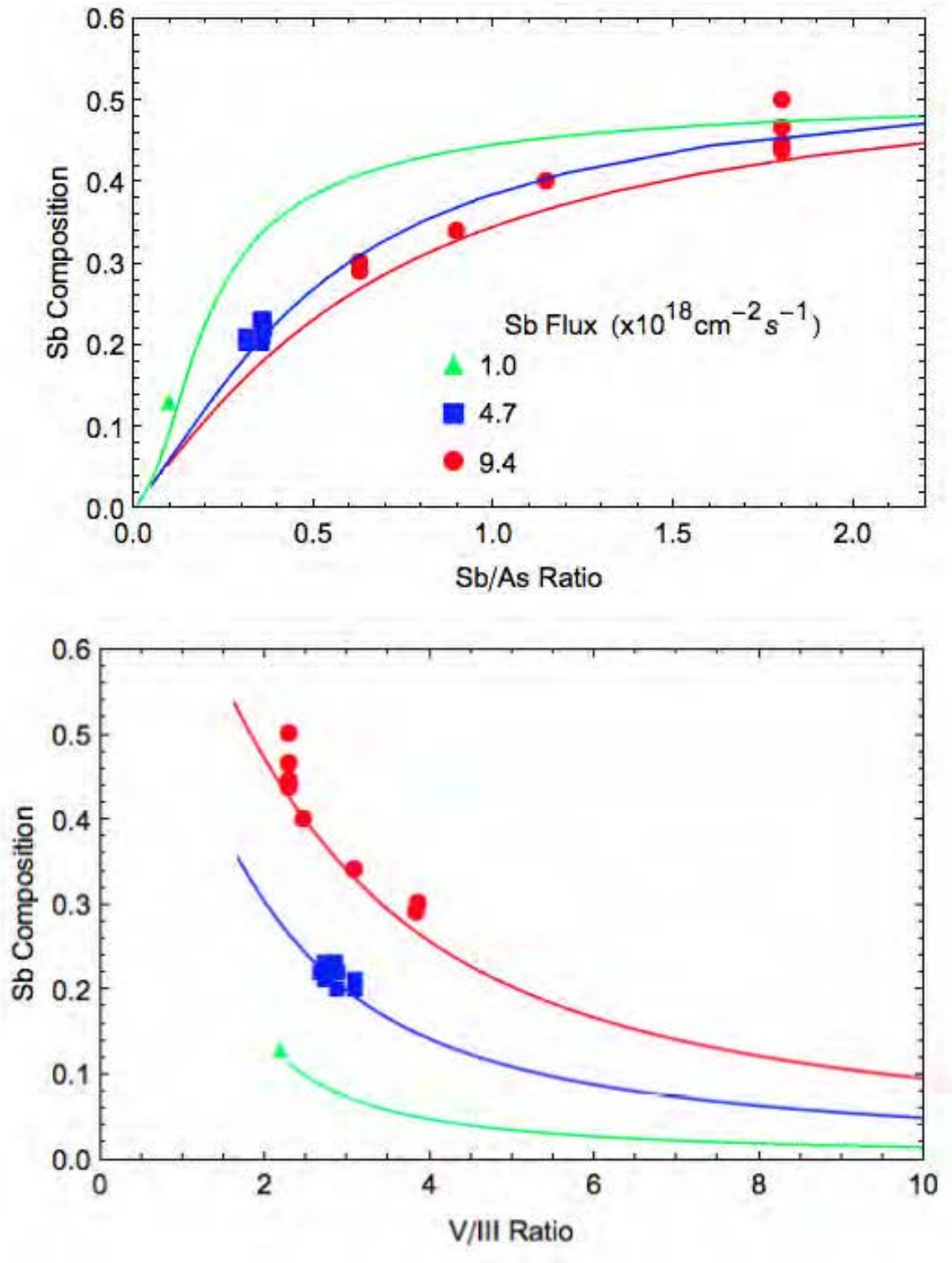

Figure 3: Sb concentration as a function of (a) Sb/As ratio and (b) V/III ratio at T=415 C for Fm= 6.3x10^18 $cm^{-2}s^{-1}$ (red and blue) and 1.0x10^18 $cm^{-2}s^{-1}$ (green). The solid lines are fits to the model using the parameters in Table 1.

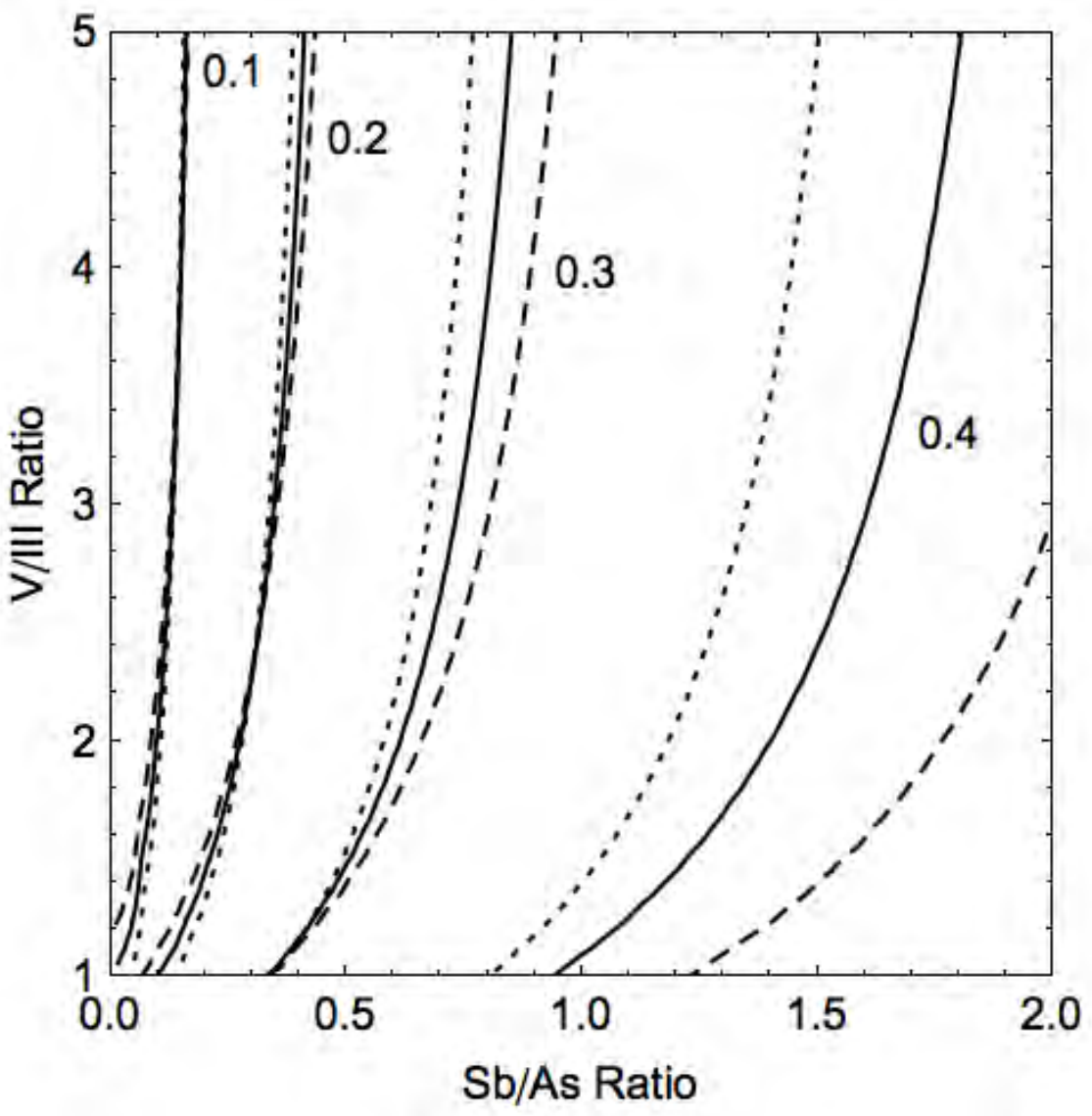

Figure 4: As and Sb fluxes required to obtain certain compositions for Fm=6.3x10^{18} $cm^{-2}s^{-1}$,T=405C (dashed), 415C (solid), and 425C (dotted).